Flexible multibody dynamics of the Enterprise amusement ride

Msc Thesis

H.G. Roubos

April 25th, 2025

Graduation committee:
Chair: Dr.ir. R.G.K.M. Aarts
Supervisor: Dr.ir. J.P. Schilder
External Member: Dr. T. Mishra

University of Twente
Faculty of Engineering Technology
Department of Applied Mechanics & Data Analysis (MS3)

Preface

Dear reader,

Thank you for being interested in my Msc thesis, 'Flexible Multibody dynamics of the Enterprise amusement ride'. Over the past few years, I have studied at the University of Twente with great enthusiasm and pleasure. Starting from the Bsc in Mechanical Engineering, I continued with interesting courses in the High Tech Systems and Materials Master track. During this time, I further challenged myself by being active in student life and in several committees Enschede has offered. But all goods must come to an end, so I started searching for my Msc graduation project. Preferably a project regarding flexible multibody dynamics or structural dynamics.
I found this in a very interesting assignment on the dynamics of the Enterprise, supervised by dr.ir. J.P. Schilder. This topic was the ideal combination of flexible multibody dynamics and structural dynamics using some experiments. Knowing Jurnan Schilder as a collaborative researcher with great explanation skills gave me the confidence to take on the challenging project.
S. Mekdachi Galayini and S. Onland started earlier on an analytical expression for the Enterprise during their Bsc thesis, of which the Bsc papers are available upon request. Together with these papers, the project evolved into a clear and complete story describing the dynamics and deformations of the Enterprise during operation. This led to the decision to present the results of the project in a journal paper and submit this for the 12th ECCOMASS Thematic Conference on Multibody Dynamics in Innsbruck, Austria. The paper is included in the following pages and will serve as the main body of this Msc thesis report.
I have written the paper in collaboration with Jurnan Schilder, where the work of Galayini and Onland served as a firm basis of the analytical model. Their work on the equation of motion of the rigid system is largely adopted and some extra analyses are made including instantaneous equilibrium situations. Jurnan Schilder was largely responsible for these derivations and the analytical model, where I assisted with evaluating the model in Matlab for the given ride sequence and preparation of figures with results.
The main aim of my Msc thesis was the development of the flexible multibody model. In order to achieve this, I created the rigid multibody model in the environment SIMCAPE and the Finite Element model of the Enterprise, including experimental verification in Attractiepark Hellendoorn. Combining those two resulted in the desired flexible multibody model. Finally, I was responsible for evaluating all four models and combining the results for post-processing and comparison of the results.
The paper has a page limit of 20 pages, therefore not offering space for everything that was studied during my Msc thesis. In order to share some additional interesting findings, these are included in the appendices to this Msc thesis report. Several pages of the paper have a footnote, referring to the corresponding appendix with extra information.
Finally, I would like to thank Saeed and Sven for their preparatory work on

the analytical expression of the Enterprise. I would also like to thank Leroy Wijering from Avonturenpark Hellendoorn and Axel Lok from the University of Twente Dynamics lab for their support and assistance during experiments on the physical Enterprise. Furthermore, I am thankful to Ronald Aarts and Tanmaya Mishra for their position in the graduation committee and my special thanks goes to Jurnan Schilder. His experience and expertise have played an important role and it was a pleasure to work with him during the project.

I hope you enjoy reading this report, do not hesitate to contact me in case of any questions or comments.

Kind regards,
Harmen Roubos

April 9th, 2025
Enschede, The Netherlands

Flexible multibody dynamics of the Enterprise amusement ride

Harmen Roubos[1], Saeed Mekdachi Galayini[1], Sven Onland[1], Jurnan Schilder[1*]

[1*]Faculty of Engineering Technology, University of Twente, P.O. Box 217, Enschede, 7500AE, The Netherlands.

*Corresponding author(s). E-mail(s): j.p.schilder@utwente.nl;
Contributing authors: h.g.roubos@student.utwente.nl;
s.mekdachigalayini@student.utwente.nl; s.onland@student.utwente.nl;

Abstract

The Enterprise is an example of an amusement ride in which passengers are subjected large motions and dynamic loads. These loads also cause continuous deformations in the structural parts of the ride. Flexible multibody dynamics models are ideal to simulate the coupled behavior of large motions and small elastic deformations. However, these models are not often used in practice, because this is not required by the current safety standards. In this work, a methodology for developing a full flexible multibody dynamic model of the Enterprise is presented and compared to both an analytical model and a rigid multibody model. Where possible, the results are validated using experimental tests on the Enterprise in Avonturenpark Hellendoorn. The results show that the flexibility of the rotating frame has very limited influence on the swinging motion of the gondola and on the g-forces on the passengers. However, the flexible model can be used to simulate the deformations of the rotating frame more realistically. The internal dynamics of the rotating frame account for approximately 10 percent of the elastic deformation of the frame. The transient simulation of these vibrations can potentially be used to further improve the assessment of static strength and fatigue strength. The methodology presented in this work can be used to study the dynamic behavior of many other amusement rides.

Keywords: Amusement rides, flexible multibody dynamics, floating frame of reference formulation, finite element method, model order reduction, Simscape multibody

1 Introduction

All over the world, amusement parks and theme parks are popular leisure destinations. The amusement rides that can be found in such parks are developed to provide an interesting experience to its passengers. The most sensational rides are known as thrill rides, which are highly dynamic multibody systems, typically with multiple axes of rotation and several degrees of freedom.

To guarantee passenger safety, the design of such machines must comply with international safety standards, such as EN 13814 [1] and Eurocode 3 [2]. Among other things, such standards prescribe ride manufacturers how to perform analyses of static strength and fatigue strength. Both types of analysis are based on quasi-static calculations of internal stresses, for which the most severe load cases are estimated.

Computational methods from the field of flexible multibody dynamics are ideal for the combined simulation of large system motions and small structural deformations. Using these methods, the full transient dynamics of an amusement ride can be simulated. In this way, excessive vibrations due to dynamic effects could be spotted and designs could become less conservative. Despite these potential benefits, flexible multibody dynamics simulations are rarely performed in the amusement ride industry. The main reason is that such an analysis is not required by the safety standards and that ride manufacturers often lack experience with the required analysis software.

In this work, it is presented how to perform a flexible multibody dynamic analysis on an amusement park ride known as the 'Enterprise', an example of which is shown in Figure 1. The ride consists of a large rotating wheel frame, constructed from 20 radial booms that are interconnected by beams. Along the circumference of the frame, 20 gondolas are connected by hinges, which gives them the ability to freely swing outward due to the rotation of the frame. Once the frame rotates at its operational velocity, the main beam lifts the frame to an almost vertical position. In this way, passengers seated in the gondolas are being continuously flipped upside down.

The original concept of the Enterprise was developed by Schwarzkopf in the 1970's. The design was then adapted and patented by Huss Park Attractions, which manufactured more than 60 rides. Inspired by the success of the Enterprise, various manufacturers developed versions with alternative seating arrangements, such as the 'Chaos' by Chance Rides in 1996, the 'Fly Away' by Huss in 2003, the 'Endeavour' by Zamperla in the 2015 and the 'Enterprise 2G' by Huss which currently exists as a concept design. Moreover, there are many other amusement rides that are somehow based on a rotating frame. Consequently, the understanding of the flexible multibody dynamics of the Enterprise is relevant for many different amusement rides.

In academic literature, most work in the field of amusement ride dynamics is concerned with roller coasters. A multibody model of a roller coaster vehicle was presented in [3] with which self-excited vibrations were analyzed. In [4], a flexible multibody model of a roller coaster vehicle was presented, based on a finite element model of a flexible chassis. In [5] and [6] the structural dynamics of the track and support structures was modeled. The literature on the multibody dynamics of thrill rides is very limited. In [7] an analytical study of the dynamic behavior of a rotating swings amusement ride was presented. In [8] a complete analysis of the flexible multibody dynamics of a fair ground ride was presented, using finite element models for slender members

Fig. 1: Enterprise in Avonturenpark Hellendoorn, The Netherlands.

and Simscape Multibody. In this work a similar approach will be used as in [8] for the multibody analysis of the Enterprise.

The linear elastic behavior of the rotating wheel frame is based on a finite element model. This model should be sufficiently detailed such that the mass- and stiffness distribution is represented well by the finite element mesh and the chosen element type(s). To minimize the computational costs of the multibody simulations, the finite element model can be reduced using linear model order reduction techniques such as Craig-Bampton [9], Rubin [10] or Herting [11]. For application in Simscape Multibody, it is convenient if the reduced order model uses the local boundary nodes in the reduced set of coordinates. Without loss of generality, a static condensation method will be used in this work, such that the local boundary nodes form the complete set of flexible coordinates.

Simscape Multibody is based on the floating frame of reference formulation to simulate flexible multibody dynamics. This formulation is commonly known in the field of multibody system dynamics and also used by other commercially available software packages. In this method, the large overall motion of each body is described by the global motion of its floating frame. Small elastic deformations are described locally, relative to the floating frame using a set of flexible coordinates corresponding to the reduced order model of the body. Kinematic constraints between different bodies are enforced by Lagrange multipliers [12].

This paper is structured as follows: In section 2, the ideal physical model of the Enterprise and the details of its ride sequence are introduced. In section 3, a simplified analytical model is presented that provides valuable insight in the overall ride dynamics. In section 4, the rigid multibody model is presented. In section 5, the (reduced) finite element model of the rotating frame is presented. In section 6, the flexible multibody model is presented. In section 7, results of the ride motion, passenger g-forces and structural deformations are presented. Simulations of the analytical model, rigid multibody and flexible multibody will be compared to discuss the added value of the increasing model complexity. The paper is finalized with the most important conclusions.

2 Ideal physical model

Figure 2 shows the ideal physical model of the Enterprise. The figure shows the inertial frame O and the coordinate frames 1, 2 and 3 that are located in the center of mass of the lifting arm, wheel frame and gondola, respectively. The figure also shows the degrees of freedom of the system: the angle of lift ψ, the angle of spin ϕ and the angle of swing θ.

The general dimensions of the Enterprise are determined from available technical documentation and measurements performed in Avonturenpark Hellendoorn. Figure 2 shows the length of the lifting arm D, the distance from the lifting arm to the center of the wheel frame H, the radius of the wheel frame R and the distance from the center of mass of the gondola to its hinge line L.

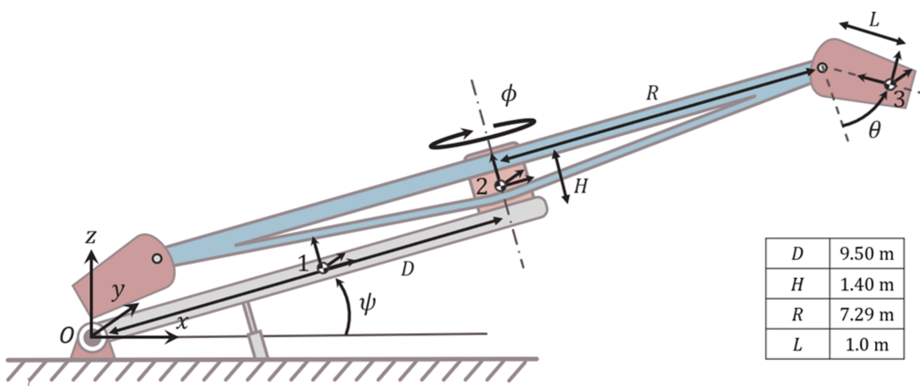

D	9.50 m
H	1.40 m
R	7.29 m
L	1.0 m

Fig. 2: Ideal physical model of the Enterprise, including its general dimensions.

Whereas D, H and R could be easily obtained from the technical documentation, the location of the center of mass of the gondola L was not precisely known. Moreover, its value would depend on whether or not passengers are seated in the gondola. When the gondola is modeled as a point mass, the natural frequency ω_0 of the swinging motion can be expressed as:

$$\omega_0 = \sqrt{\frac{g}{L}} \tag{1}$$

in which g is the gravitational acceleration. A realistic value for L is obtained from the measured damped free vibration response of an empty gondola, shown in figure 3. Due to the presence of dry friction and nonlinear dampers, the response differs from an idealized viscously damped response. Nevertheless, in this figure a natural frequency of approximately 0.5 Hz can be observed, which corresponds to an equivalent length L of approximately 1.0 m.

The mass of the gondola m is also not known, as the technical documentation only contains information on the structural frame of the gondola, not taking into account the plastic seating compartment and restraint frames. To obtain a realistic value for

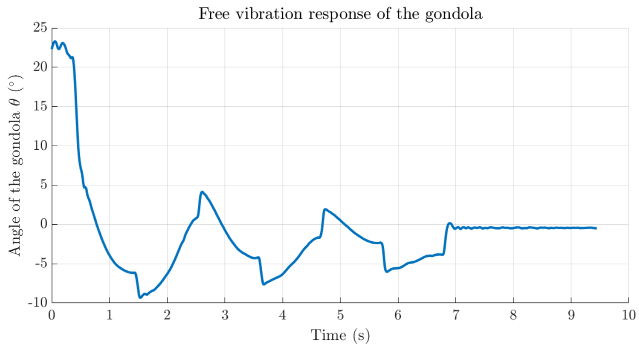

Fig. 3: Free vibration response of a gondola.

its mass, one empty gondola of the Enterprise in Avonturenpark Hellendoorn was weighted. From this it is found that the $m = 194$ kg.

The Enterprise is driven by the hydraulic motors of the lifting arm and wheel frame. The ride control system effectively ensures that the angle of lift ψ and the angle of spin ϕ follow a predefined ride sequence. Since the exact ride sequence may differ slightly for each Enterprise ride, a reference ride sequence is constructed from measurements performed in Avonturenpark Hellendoorn. In particular, the speeding up and slowing down of the lifting arm and wheel frame are obtained from the park.

The ride sequence starts by speeding up the spinning wheel frame to a constant angular velocity Ω of 1.55 rad/s. Once this value is reached, the lifting arm raises to its upright position of 76°. The lifting arm remains in this position for a certain time and then lowers again. Once the arm is in its downward position, the wheel frame slows down to a complete stop. Figure 4 visualizes the ride sequence that is defined mathematically by the following step functions for the angular accelerations:

$$\ddot{\phi}(t) = \begin{cases} 0.062 & \text{if } 0 < t \leq 25 \\ -0.062 & \text{if } 155 \leq t < 180 \\ 0 & \text{otherwise} \end{cases} \qquad \ddot{\psi}(t) = \begin{cases} 0.02 & \text{if } 25 < t \leq 27 \\ -0.02 & \text{if } 58 < t \leq 60 \\ -0.015 & \text{if } 108 < t \leq 110 \\ 0.015 & \text{if } 153 < t \leq 155 \\ 0 & \text{otherwise} \end{cases} \tag{2}$$

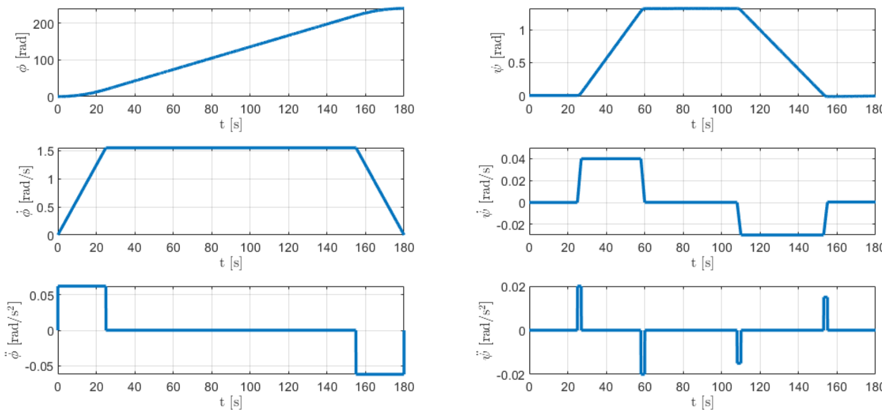

Fig. 4: Prescribed angle of spin ϕ (left) and angle of lift ψ (right) of the ride sequence.

3 Analytical model

When it is assumed that all bodies are rigid and that the motions of the lifting arm and rotating frame are prescribed, the motions of the gondolas do not influence each other. Under these assumptions, the equation of motion of a freely swinging gondola can be derived analytically. Using Figure 2, the following (relative) rotation matrices can be defined in terms of the coordinates ψ, ϕ and θ:

$$\mathbf{R}_1^O = \begin{bmatrix} \cos\psi & 0 & -\sin\psi \\ 0 & 1 & 0 \\ \sin\psi & 0 & \cos\psi \end{bmatrix}, \quad \mathbf{R}_2^1 = \begin{bmatrix} \cos\phi & \sin\phi & 0 \\ -\sin\phi & \cos\phi & 0 \\ 0 & 0 & 1 \end{bmatrix}, \quad \mathbf{R}_3^2 = \begin{bmatrix} \cos\theta & 0 & -\sin\theta \\ 0 & 1 & 0 \\ \sin\theta & 0 & \cos\theta \end{bmatrix} \tag{3}$$

In this notation, $\mathbf{R}_j^i$ denotes the orientation of frame j relative to frame i. The absolute position of the center of mass of the gondola $\mathbf{r}_3^{O,O}$ can be expressed as:

$$\mathbf{r}_3^{O,O} = \begin{bmatrix} x_3^{O,O} \\ y_3^{O,O} \\ z_3^{O,O} \end{bmatrix} = \mathbf{R}_1^O \begin{bmatrix} D \\ 0 \\ H \end{bmatrix} + \mathbf{R}_1^O\mathbf{R}_2^1 \begin{bmatrix} R \\ 0 \\ 0 \end{bmatrix} + \mathbf{R}_1^O\mathbf{R}_2^1\mathbf{R}_3^2 \begin{bmatrix} 0 \\ 0 \\ -L \end{bmatrix} \tag{4}$$

In this notation, $\mathbf{r}_j^{k,i}$ denotes the position vector of point j relative to point i and its components are expressed in frame k. The rotation matrices from equation (3) can be substituted in equation (4). Differentiation with respect to time yields an expression for the absolute velocity $\dot{\mathbf{r}}_3^{O,O}$ of the center of mass of the gondola. With this, the Lagrangian $\mathcal{L}$ can be obtained:

$$\mathcal{L} = \frac{1}{2}m\left((\dot{x}_3^{O,O})^2 + (\dot{y}_3^{O,O})^2 + (\dot{z}_3^{O,O})^2\right) - mgz_3^{O,O} \tag{5}$$

The equation of motion is derived from Lagrange's equation:

$$\frac{d}{dt}\left(\frac{\partial \mathcal{L}}{\partial \dot{\theta}}\right) - \frac{\partial \mathcal{L}}{\partial \theta} = 0 \tag{6}$$

With some arithmetic, it can be shown that the resulting equation of motion equals:

$$\begin{aligned} &\ddot{\theta}L + \ddot{\psi}\{(L + R\sin\theta - H\cos\theta)\cos\phi + D\sin\theta\} \\ &\quad - \dot{\psi}^2\{(D + R\cos\phi)\cos\phi\cos\theta + (L\sin^2\phi\cos\theta - H)\sin\theta\} - \dot{\phi}^2(R + L\sin\theta)\cos\theta \\ &\quad + 2\dot{\psi}\dot{\phi}(L\cos^2\theta - L - R\sin\theta)\sin\phi + g(\sin\psi\cos\phi\cos\theta + \cos\psi\sin\theta) = 0. \end{aligned} \tag{7}$$

This equation of motion can be interpreted as a second order differential equation for θ, with ψ and ϕ prescribed functions in time. One can recognize terms due to the angular accelerations $\ddot{\theta}$ and $\ddot{\psi}$, centripetal accelerations $\dot{\psi}^2$ and $\dot{\phi}$, Coriolis acceleration $2\dot{\psi}\dot{\phi}$ and the gravitational acceleration g.

The equation of motion (7) can be simplified for analytical purposes, by considering that for the majority of the ride sequence the angular velocity of the wheel frame $\dot{\phi} = \Omega$ is constant. Moreover, the angular acceleration of the lifting arm is mostly zero $\ddot{\psi} = 0$ and its operational velocity is very low in comparison to the natural frequency of the swinging motion: $\dot{\psi} \ll \omega_0$. With this, the equation of motion reduces to:

$$\ddot{\theta} - \Omega^2\left(\frac{R}{L} + \sin\theta\right)\cos\theta + \omega_0^2\left(\sin\psi\cos\phi\cos\theta + \cos\psi\sin\theta\right) = 0 \tag{8}$$

Note that this equation of motion does no longer depend on the dimensions of the lifting arm D and H. The dynamic behavior of the swinging motion only depends on the ratio R/L, the angular velocity of spin Ω, the instantaneous angle of lift ψ that defines the inclination of the wheel frame, and the instantaneous angle of spin ϕ.

When dynamic effects are ignored, one can determine the *instantaneous equilibrium angle of swing* θ_{eq} from the following equation of equilibrium:

$$-\Omega^2\left(\frac{R}{L} + \sin\theta_{eq}\right)\cos\theta_{eq} + \omega_0^2\left(\sin\psi\cos\phi\cos\theta_{eq} + \cos\psi\sin\theta_{eq}\right) = 0 \tag{9}$$

Figure 5 shows the instantaneous equilibrium angle of swing as a function of the angle of spin ϕ of the wheel frame for several values of the angle of lift ψ. It can be seen that when the lifting arm is in its horizontal position, the equilibrium angle of swing is constant and equal to 63.5°. When the lifting arm is fully upright, the equilibrium angle of swing is constant and equal to 90°. However, during the lifting motion, the angle of swing is not constant. This means that the swinging motion of the gondola during the lift is fundamental in nature. Hence, transient dynamics or disturbances are not strictly necessary to explain the swinging motion that is observed in practice.

The natural frequency of the swinging motion is affected by the lifting of the arm and the rotation of the wheel. In order to derive an expression for the *instantaneous natural frequency* ω_n, the equation of motion (8) is linearized about the instantaneous

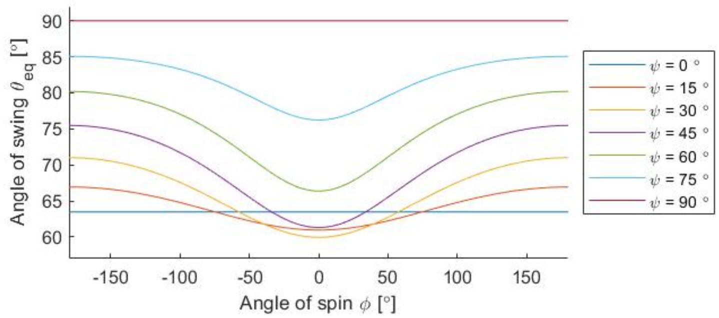

Fig. 5: Instantaneous equilibrium angle of swing θ_{eq} as a function of the angle of spin ϕ for several values of the angle of lift ψ.

equilibrium angle of swing θ_{eq}. Consider that the angle of swing can be written as $\theta = \theta_{eq} + \Delta\theta$, in which $\Delta\theta$ is the angle of swing relative to the instantaneous equilibrium angle. For small motions values of $\Delta\theta$, the trigonometric functions in θ in the equation of motion (8) can be linearized. Applying the the equilibrium condition (9) yields the following linearized equation of motion:

$$\Delta\ddot{\theta} + \omega_0^2 \left((\cos\psi \cos\theta_{eq} - \sin\psi \cos\phi \sin\theta_{eq}) + \frac{\Omega^2}{\omega_0^2} \left(\frac{R}{L} \sin\theta_{eq} - \cos(2\theta_{eq}) \right) \right) \Delta\theta = 0 \tag{10}$$

From this, the instantaneous natural frequency ω_n can be determined:

$$\omega_n = \omega_0 \sqrt{\left(\cos\psi \cos\theta_{eq} - \sin\psi \cos\phi \sin\theta_{eq} + \frac{\Omega^2}{\omega_0^2} \left(\frac{R}{L} \sin\theta_{eq} - \cos(2\theta_{eq}) \right) \right)} \tag{11}$$

Figure 6 shows the dimensionless instantaneous frequency ω_n/ω_0 as a function of the angle of spin ϕ for several values of the angle of lift ψ. When the lifting arm is in its downward position, the natural frequency of the swinging motion has increased from 0.5 Hz to 0.74 Hz, due to the spinning of the wheel frame. When the lifting arm is fully upright, the instantaneous natural frequency varies between 0.51 Hz and 0.87 Hz.

When determining the forces exerted on the passengers, it is standard practice to determine do this in the so-called passenger coordinate frame P, in which the local x-axis is forward, the local y-axis is to the left and the local z-axis is up. The passenger coordinate frame P can be obtained by rotating frame 3 about its z-axis $-90°$. Let $\mathbf{R}_3^P$ denote the rotation matrix that performs this transformation. The local passenger force vector $\mathbf{F}^P$ can be determined from Newton's second law:

$$\mathbf{F}^P = \mathbf{R}_3^P \mathbf{R}_2^3 \mathbf{R}_1^2 \mathbf{R}_O^1 \left(m\ddot{\mathbf{r}}_3^{O,O} - m\mathbf{g}^O \right) \tag{12}$$

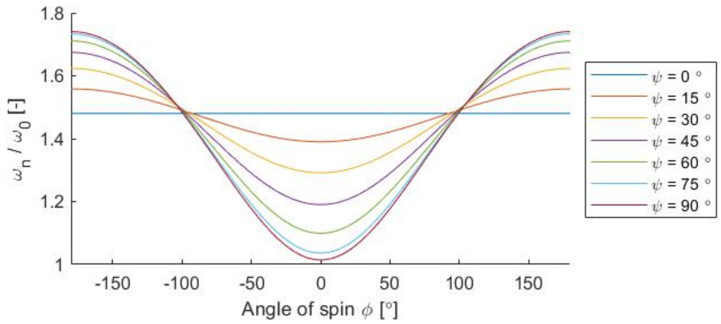

Fig. 6: Dimensionless instantaneous natural frequency ω_n/ω_0 of the swinging motion as a function of the angle of spin ϕ for several values of the angle of lift ψ.

in this, $\ddot{\mathbf{r}}_3^{O,O}$ is the acceleration of the center of mass of the gondola, which is obtained by differentiating equation (4) with respect to time twice and $\mathbf{g}^O = [0 \;\; 0 \;\; -g]^T$ is the global gravitational acceleration vector.

Because the instantaneous equilibrium angle of swing already gives a good idea of the motion of the gondola, it is of interest to determine the so-called *instantaneous equilibrium passenger force vector* $\mathbf{F}_{eq}^P$. This can be done by applying the equilibrium conditions from equation (9) to equation (12), which yields:

$$\mathbf{F}_{eq}^P = mg \begin{bmatrix} -\sin\psi\sin\phi \\ 0 \\ \frac{\Omega^2}{g}(R + L\sin\theta_{eq})\sin\theta_{eq} + \cos\psi\cos\theta_{eq} - \sin\psi\cos\phi\sin\theta_{eq} \end{bmatrix} \tag{13}$$

Note that by isolating mg in equation (13), the terms in the vector are dimensionless. The components in this dimensionless passenger force vector are commonly referred to as the *g-forces* experienced by the passenger.

It can be seen that in the local y-direction, the passenger does not experience any force. This is logical, because by definition of the instantaneous equilibrium angle, the gondola is oriented such that it does not swing sideways. In the local x-direction, there is only a component of gravity. When this force is positive, it represents the force by the back support onto the passenger's back. When it is negative, it represents the force by the foot stands onto the passenger's feet and/or the friction force between the seat and the passenger. In the local z-direction, there is a component due to the rotation of the wheel frame and a component of gravity. The ride must rotate sufficiently fast for this term to always remain positive, otherwise the passenger would come loose from the seat, resulting in an unsafe situation. Figure 7 shows the z-component of the instantaneous equilibrium passenger g-force as a function of the angle of spin ϕ for several values of the angle of lift ψ. It can be seen that when the lifting arm is in its horizontal position, the g-force is constant and equal to 2.2. When the lifting arm is fully upright, the g-force varies between 1.0 and 3.0.

Note: Full expressions for passenger accelerations in frame 3 and frame P are available in appendix A

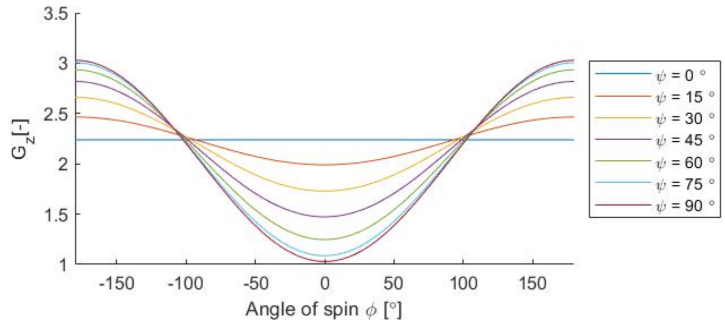

Fig. 7: Instantaneous equilibrium vertical g-force on the passenger as a function of the angle of sping ϕ for several values of the angle of lift ψ.

4 Rigid multibody model

The multibody model is set up in Simscape Multibody environment, using a simplified geometry, which is shown in figure 8. The rigid bodies of the lifting arm, wheel frame and gondolas are modeled using solid elements. For the purpose of visualization, the geometry of these models is imported. Each body is given its rigid body inertia properties.

The bodies are connected to each other by means of joints. The connections between the fixed world and the lifting arm and between the lifting arm and the wheel frame are both modeled by a revolute joint. Each gondola is connected to the wheel frame in two interface points. One interface is modeled by a spherical joint, only connecting the origins of the interface frames. A so-called telescopic joint is present at the second interface point. This joint provides an additional degree of freedom in the translational direction from interface point to interface. In this way overconstraining is avoided. The degrees of freedom of each of the used joints are visible in figure 9.

The implementation of the ride sequence, as described in section 2, is carried out by prescribed angles and angular velocities for two revolute joints. To avoid problems with numerical instable behavior during the transient simulation, a small amount of spherical damping of 5 Nms/deg is specified in the spherical and telescopic joints of each of the gondolas.

Simscape Multibody is based on the floating frame of reference formulation. In this rigid multibody model, a floating frame is rigidly attached to the center of mass of each body. The generalized coordinates $\mathbf{q}$ are the coordinates related to the global position and angular parametrization of these frames. Based on the selected joints, a vector of holonomic kinematic constraint equations $\mathbf{C}_k(\mathbf{q}) = \mathbf{0}$ is created. The prescribed motions of the ride sequence results in two driving constraint equations of the form $\mathbf{C}_d(\mathbf{q}, t) = \mathbf{0}$. Based on this the constrained equations of motion of the rigid multibody model in standard form are obtained:

$$\begin{bmatrix} \mathbf{M} & \mathbf{C}_q^T \\ \mathbf{C}_q & \mathbf{0} \end{bmatrix} \begin{bmatrix} \ddot{\mathbf{q}} \\ \lambda \end{bmatrix} = \begin{bmatrix} \mathbf{Q}_a \\ \gamma \end{bmatrix} \tag{14}$$

Note: An overview of the Simscape *diagram model is present in appendix B*

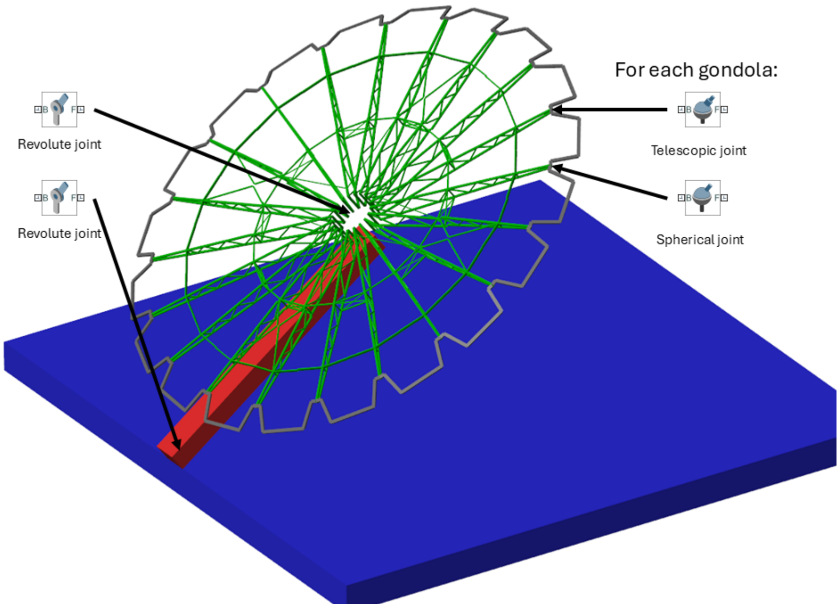

Fig. 8: Simscape Multibody model of the Enterprise.

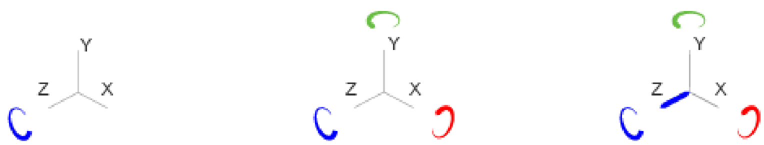

(a) Revolute Joint (b) Spherical Joint (c) Telescopic joint

Fig. 9: The degrees of freedom for each of the used Simscape joints.

where $\mathbf{M}$ is the mass matrix of the multibody system, $\mathbf{C}_q$ is the Jacobian of the constraint equations, λ are the Lagrange multipliers enforcing the constraints, $\mathbf{Q}_a$ is the vector of applied forces (which only contains gravitational forces), and γ is the right hand side of the acceleration equation of the constraints.

5 Finite element model

The structural finite element model of the Enterprise is created in software package Ansys. For the purpose of this work, only the flexibility of the wheel frame is considered. Because the wheel frame is designed using slender members only, the geometry of the frame is simplified to a so-called wire frame of 1D line bodies. Cross-sectional properties are assigned to each of the line bodies, representing their truss member type. In figure 10, the different cross-sectional properties for truss members are visualized. In ANYS DESIGNMODELER, the 'shared topology' function is used to model a fixed connection between line bodies, resulting in a complete truss structure geometry used for further analysis.

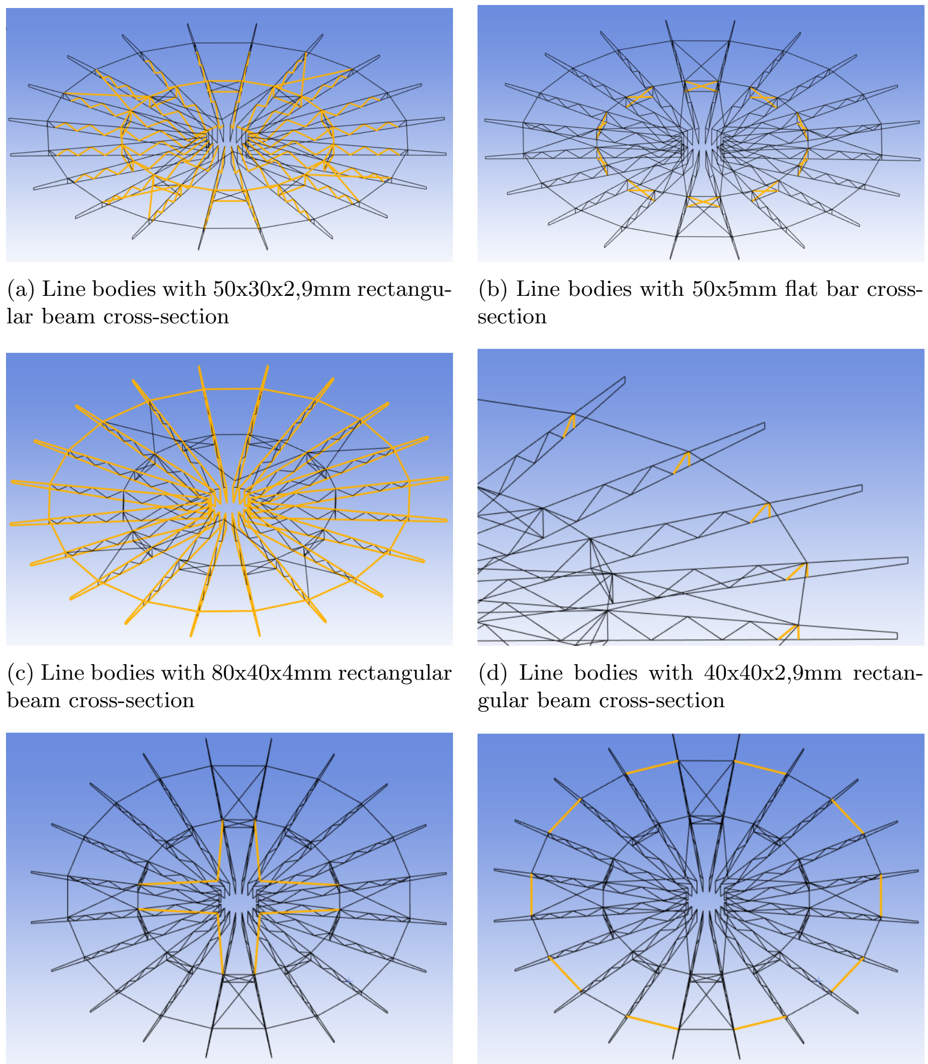

(a) Line bodies with 50x30x2,9mm rectangular beam cross-section

(b) Line bodies with 50x5mm flat bar cross-section

(c) Line bodies with 80x40x4mm rectangular beam cross-section

(d) Line bodies with 40x40x2,9mm rectangular beam cross-section

(e) Line bodies with 38mm round bar cross-section

(f) Line bodies with 16mm round beam cross-section

Fig. 10: Cross-sectional properties of the 1D line bodies of the wheel frame.

The finite element model is build from two types of elements. For most line bodies, a 1D BEAM element is used, which has 6 nodal degrees of freedom per node. As most of the truss members are welded together, these elements are necessary to transfer axial, torsional and bending loads. Some of the truss members in the frame are connected by two hinges instead of welds. For long slender members where this is the case, the beam element is not representative as it should not be able to transfer any rotational loads in the nodes. In these cases, the LINK180 element is used, which is a 1D BAR element that can only transfer axial loads. In addition, the hinged truss members consist of only 1 element, to prevent buckling of multiple LINK180 elements when subjected to compressive load. Figure 11 shows an overview of the elements used. The full model consists of 1472 elements and 2766 nodes.

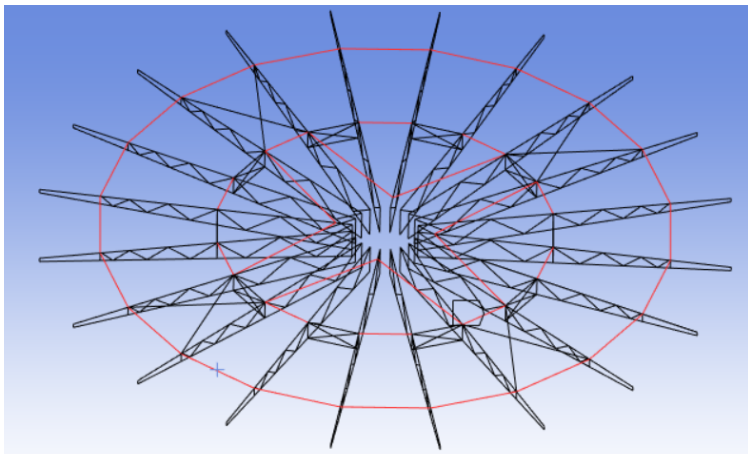

Fig. 11: Line body model of the wheel frame, where standard 1D BEAM elements and 1D BAR elements are indicated in black and red, respectively.

A modal analysis is performed on the full finite element model in order to determine the natural frequencies and corresponding natural modes of the non-rotating frame. The frame booms are rigidly fixed to the reference world at the center pivot, after which the first 5 natural frequencies and corresponding modes are computed. These modes are visible in figure 12. As the center pivot is fixed in the modal analysis, the first mode consists of a torsional mode around the center axis. However, in reality the wheel frame can rotate about the local z-axis, which is why this mode will not be found during experimental verification. Modes 2 to 5 represent bending modes of the frame at a frequency of approximately 4.5 Hz.

Figure 13 shows the frequency response functions that are obtained from the four sensors measurements. It is observed that the experimental natural frequencies are at 1.6, 2.2, 4.0 and 4.35 Hz. By analyzing the phase differences between the sensors, it is possible to reconstruct to which natural modes these natural frequencies correspond.

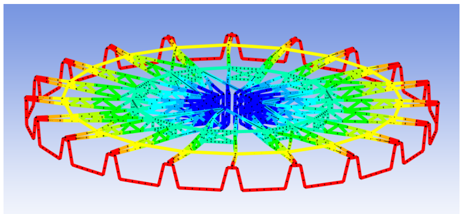

(a) Mode shape 1

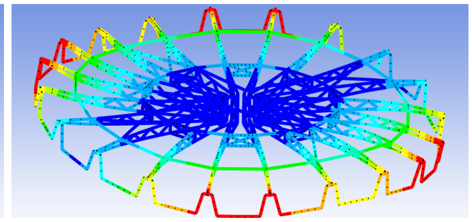

(b) Mode shape 2

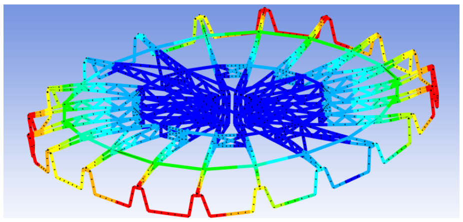

(c) Mode shape 3

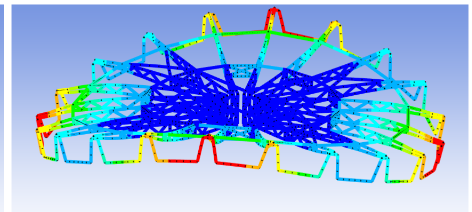

(d) Mode shape 4

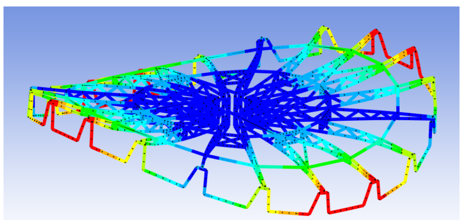

(e) Mode shape 5

Mode number	frequency [Hz]
1	2.09
2	4.44
3	4.44
4	4.47
5	4.53

Fig. 12: Natural modes 1 to 5 according to ANSYS Modal Analysis.

Modes 2 and 3 show a deformation where half the frame is moving upwards and the other half is moving downward. In the experiments, these modes have a lower natural frequency than in the finite element model: 1.6 and 2.2 Hz instead of 4.44 Hz. An explanation for this difference is found in the flexibility of the main beam. As these modes create significant torque on the central revolute joint, the main beam shows rotational deformation. Because the main beam is modeled as a rigid connection in the finite element model, this model overestimates the natural frequencies.

Modes 4 and 5 correspond to the saddle shaped modes. In experiments the natural frequencies of these modes are around 4.0 and 4.35 Hz, which is reasonably close to the finite element model. The model is more accurate for these modes, because the central hub does not deform, such that modeling the main beam as a rigid connection is an accurate representation of reality for these modes.

For the purpose of implementation in SIMSCAPE MULTIBODY, a reduced order model is created from the full finite element model. To this end, an ANSYS 'Substructure generation' analysis is used for computing reduced stiffness- and mass matrices.

Note: Additional figures and description on the experiments can be found in appendix C

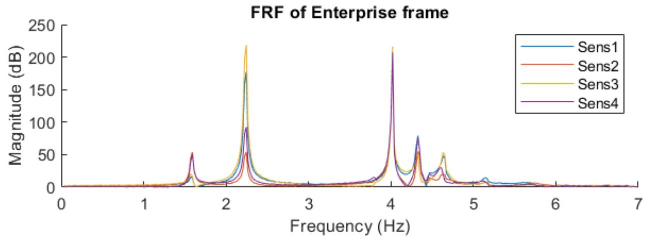

Fig. 13: Experimentally determined frequency response functions of the wheel frame.

This analysis is based on the Craig-Bampton model order reduction method. In this analysis, 22 boundary nodes were taken into account for the static condensation: these are the 20 interface points between the wheel frame and the gondolas and 2 remote points at the center of all booms, representing the rotating interface between the wheel frame and lifting arm. No internal vibration modes are taken into account. The reduced order model that is obtained in this way has 132 degrees of freedom instead of 16596 of the full model.

6 Flexible multibody model

The rigid multibody model in Simscape Multibody that was introduced in Section 4, is expanded to incorporate the flexible behavior of the wheel frame. To this end, the reduced mass and stiffness matrices are exported from Ansys, together with information on the coordinates of the interface points. This information is imported in the 'Reduced Order Flexible Model' block in Simscape Multibody. In addition, the damping of the model needs to be specified. This can be of the form Modal, Proportional, or via a damping matrix. In this work, a modal damping value of 0.1 is used. Although the actual damping of the natural modes of the wheel frame are probably lower than 0.1, this amount of damping seemed necessary to avoid numerical instabilities and excessive computational times.

The fact that the wheel frame is now flexible, the set of generalized coordinates $\mathbf{q}$ of the original model is augmented with a set of flexible coordinates, which are the local coordinates of the interface points, measured relative to the floating frame of the wheel frame. The number of kinematic constraint equations $\mathbf{C}_k(\mathbf{q}) = \mathbf{0}$ remains the same, yet these equations are updated to accommodate the flexibility of the wheel frame. The constrained equations of motion of the flexible multibody systems can be written as:

$$\begin{bmatrix} \mathbf{M} & \mathbf{C}_q^T \\ \mathbf{C}_q & \mathbf{0} \end{bmatrix} \begin{bmatrix} \ddot{\mathbf{q}} \\ \lambda \end{bmatrix} = \begin{bmatrix} \mathbf{Q}_a - \mathbf{D}\dot{\mathbf{q}} - \mathbf{K}\mathbf{q} \\ \gamma \end{bmatrix} \tag{15}$$

The generalized accelerations are solved from the equations of motion (15). The generalized coordinates at the next time step are obtained from numerical time integration. At the next time step, a Newton-Raphson procedure is used to enforce the kinematic constraints on position level, with the solver consistency tolerance parameter set to 0.005.

Note: An overview of the Simscape *diagram model is present in appendix B*

7 Results & discussion

Figure 14 shows the results for the angle of swing $\theta(t)$ and its time derivatives during the complete ride sequence, as obtained from various models:

- The instantaneous equilibrium angle of swing, as solved from equation (9).
- The angle of swing as solved from the analytical equation of motion (7).
- The angle of swing as solved from the rigid multibody model in Simscape.
- The angle of swing as solved from the flexible multibody model in Simscape.

It can be seen that the analytical model and the rigid multibody model show very similar results. The instantaneous equilibrium angle also gives a very good approximation of the angle of swing, but it lacks swinging motion in the natural frequency ω_n of the gondola. The analytical model and the rigid multibody model both describe these oscillations. The flexibility of the frame has very limited influence on the angle of swing. However the effect of the flexibility dominates the acceleration plot, due to the fact that these vibrations occur at high frequencies.

Figure 15 shows the g-forces on the passenger in x-, y- and z-direction using the same four models as above. It can be seen that generally all models produce similar results. The g-force in x-direction varies between $+1$ and -1, which is only due to the changing component of gravity. The g-force in z-direction varies between 1 and 3, due to the rotating of the wheel frame. The dynamic effects of the swinging of the gondola does not seem to have a significant effect on the g-forces in these directions. However, it can be seen that the g-force in y-direction is influenced by the dynamic oscillations of the gondola. Whereas the instantaneous equilibrium analysis predicts zero lateral forces, it follows from the analytical analysis and the rigid multibody model, that the swinging of the gondola causes lateral g-forces between $+0.2$ and -0.2.

The flexibility of the wheel frame does not seem to have a large impact on the passenger g-forces as the results of the flexible multibody model correspond well to the other simulations. However, clear vibrations can be seen around abrupt changes in the ride sequence, for example when the wheel frame starts to spin and when the lifting arm starts to raise. These vibrations can be reduced by smoothening the transitions in the ride sequence, but because these vibrations are relatively small anyway, this is of not much practical importance.

Figure 16 shows the deflection in z-direction of an interface point between the frame and gondolas as obtained from the flexible multibody model. The ride sequence starts from a static deformation of 11.2 mm, which was confirmed with a static structural analysis in Ansys. The figure shows that the deformation changes in a frequency corresponding to the rotational frequency of the wheel frame. Superimposed are deformations with a higher frequency, due to the internal dynamics of the wheel frame. From this analysis it follows deformations due to the rotation of the frame are in the order of 5 mm, whereas the deformations due to the dynamic behavior of the frame are in the order of 0.5 mm.

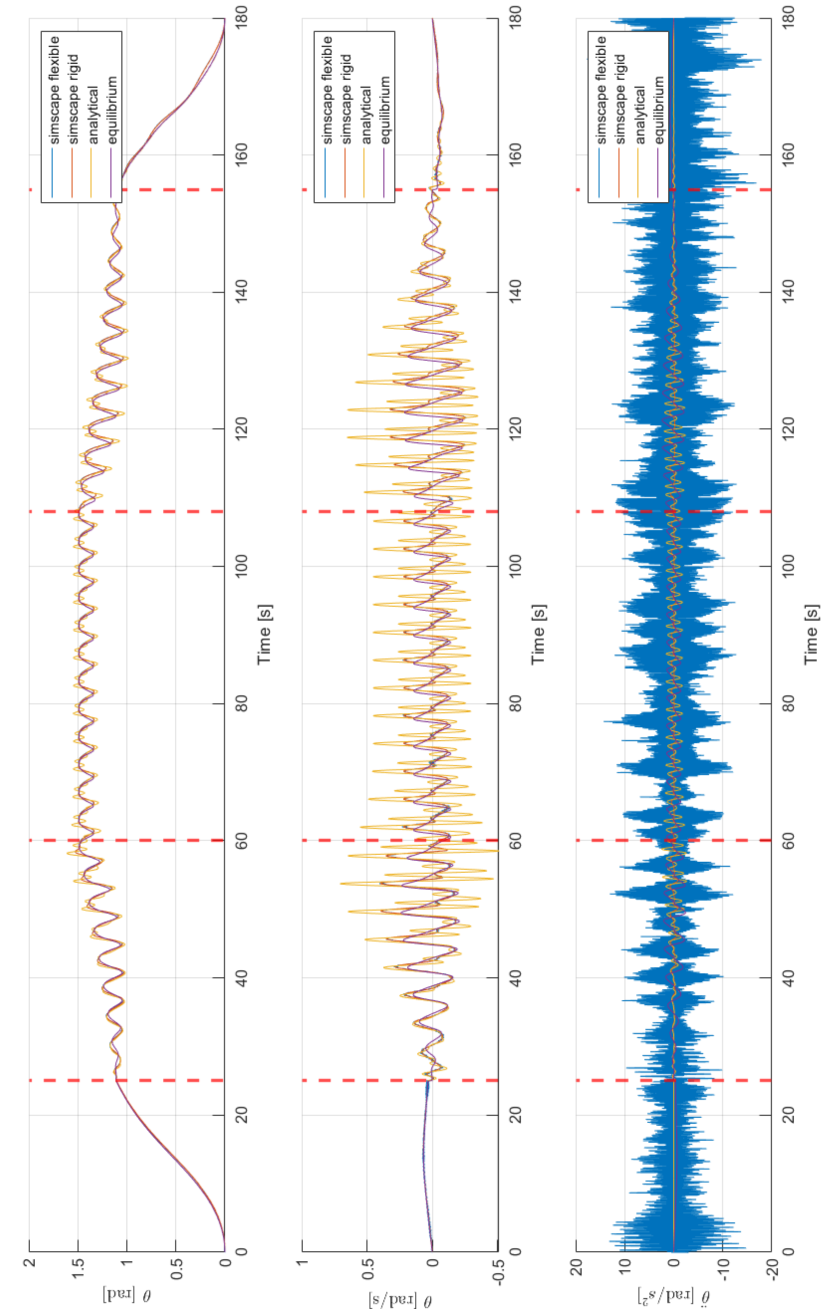

Fig. 14: Angle of swing θ and its time derivatives during the ride sequence.

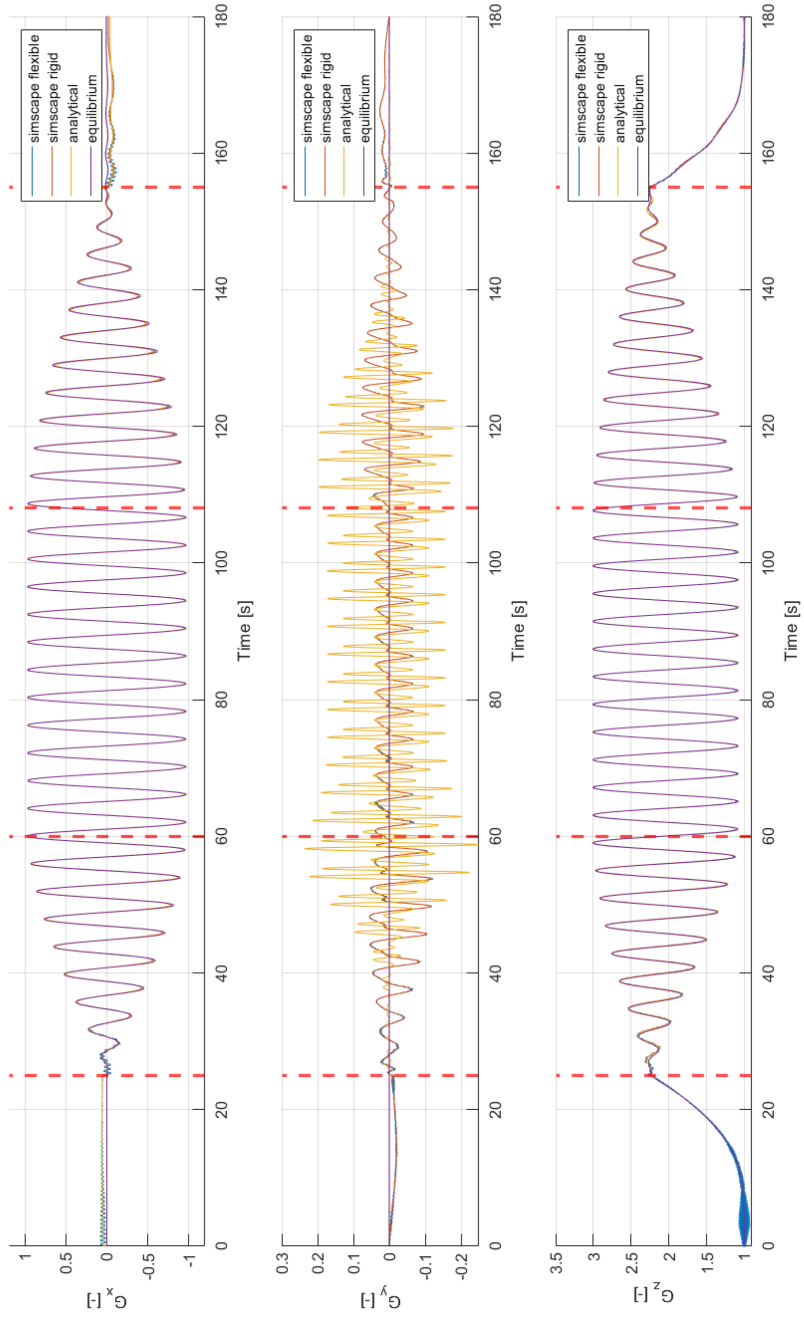

Fig. 15: Passenger g-forces in accelerations during the ride sequence.

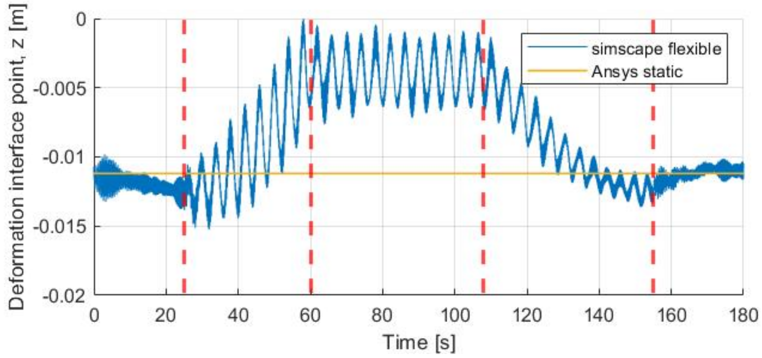

Fig. 16: Local vertical deformation of an interface point between the gondola and wheel frame during ride sequence.

8 Conclusion

Based on the analytical analysis in this work, it can be concluded that equilibrium angle of swing of a gondola is not constant during a rotation of the wheel frame. This means that the swinging motion of the gondolas are intrinsic to the natural of the Enterprise.

Assuming the gondola to be always in its instantaneous equilibrium is a very reasonable approximation, because the motion of the lifting arm is sufficiently slow and the frequency of the rotation of the wheel frame is low in comparison to the natural frequency of the swinging motion. However, from the rigid multibody model, it can be seen that the gondola swings in its natural frequency and this causes some small lateral g-forces.

The effect of the flexibility of the wheel frame on the angle of swing of the gondola and passenger g-forces can generally be ignored. Hence, for the purpose of analyzing the overall motion of the Enterprise and the forces on the passengers, rigid multibody models suffice.

However, the internal dynamics of the wheel frame cause structural deformations of approximately 10 percent of the total deformation. Despite the relative low magnitude of these deformations, they occur at relatively high frequencies of 1.6 to 4.35 Hz. In order to judge the effect of these vibrations on the structural integrity of the ride, a proper analysis of the static strength and fatigue strength should be performed.

The methodology as presented in this work for the Enterprise, can easily be adapted to numerous other amusement rides. The use of flexible multibody dynamics models provide more realistic results for the structural deformations than conventional quasi-static approximations. Concluding, in any case in which a more detailed description of ride dynamics is desired for the purpose of structural assessment, developing flexible multibody dynamics models is the way forward.

References

[1] EN13814: Safety of amusement rides and amusement devices (2019)

[2] EN1993: Eurocode 3, Design of steel structures. Part 1-8: Design of joints and Part 1-9: Fatigue (1993)

[3] Guillem Zamora Agustí, M., Kecskeméthy, A.: Self-excitability of roller coasters trains along spatial trajectories. Paper presented at the 11th ECCOMAS Thematic Conference on Multibody Dynamics (2023)

[4] Cianetti, F., Braccesi, C., Landi, L.: Integrated Roller Coaster Design Environment: Dynamic and Structural Vehicle Analysis. Paper presented at the International Mechanical Engineering Congress Exposition IMECE2015 (2015)

[5] Braccesi, C., Cianetti, F.: Development of a procedure for the structural design of roller coaster structures: The rails. Engineering Structures **93**, 13–26 (2015)

[6] Braccesi, C., Cianetti, F.: Development of a procedure for the structural design of roller coaster structures: The supporting structures. Engineering Structures **168**, 643–652 (2018)

[7] Schilder, J., Pendrill, A.: The coriolis effect and coupled oscillations in a rotating swings amusement ride. European journal of physics **45**(2) (2024)

[8] Blaauw, J., Schilder, J.: Structural analysis of a swinging fairground attraction using a novel implementation of reduced order modeling in multibody dynamics. Engineering Structures **253** (2022)

[9] Craig, R.R., Bampton, M.C.C.: Coupling of substructures for dynamic analyses. AIAA J. **6**(7), 1313–1319 (1968)

[10] Rubin, S.: Improved component-mode representation for structural dynamic analysis. AIAA J. **13**(8), 995–1006 (1975)

[11] Herting, D.N.: A general purpose, multi-stage, component modal synthesis method. Finite Elem. Anal. Des. **1**(2), 153–164 (1985)

[12] Shabana, A.A.: Dynamics of Multibody Systems. Cambridge University Press, Cambride (1998)

A Analytical passenger accelerations

Below, the full expressions for passenger accelerations in frame 3 and frame P are defined. Starting with the accelerations in frame 3:

$$\ddot{r}_3^{3O} = \begin{bmatrix} L\ddot{\theta} - R\cos\theta\dot{\phi}^2 + L\cos\phi\ddot{\psi} - H\sin\theta\dot{\psi}^2 + D\sin\theta\ddot{\psi} - \frac{L}{2}\sin 2\theta\dot{\phi}^2 + \frac{L}{2}\sin 2\theta\dot{\psi}^2 \\ -D\cos\phi\cos\theta\dot{\psi}^2 - H\cos\phi\cos\theta\ddot{\psi} - 2L\sin\phi\dot{\phi}\dot{\psi} + R\cos\phi\sin\theta\ddot{\psi} \\ -R\cos^2\phi\cos\theta\dot{\psi}^2 - L\cos^2\phi\cos\theta\sin\theta\dot{\psi}^2 + 2L\cos^2\theta\sin\phi\dot{\phi}\dot{\psi} - 2R\sin\phi\sin\theta\dot{\phi}\dot{\psi} \\ \\ L\cos\theta\sin\phi\ddot{\psi} - D\sin\phi\dot{\psi}^2 - H\sin\phi\ddot{\psi} - L\sin\theta\ddot{\phi} - \frac{R}{2}\sin 2\phi\dot{\psi}^2 \\ -2L\cos\theta\dot{\phi}\dot{\theta} - R\ddot{\phi} - L\cos\phi\sin\phi\sin\theta\dot{\psi}^2 - 2L\sin\phi\sin\theta\dot{\psi}\dot{\theta} \\ \\ L\dot{\phi}^2 + L\dot{\theta}^2 - H\cos\theta\dot{\psi}^2 + D\cos\theta\ddot{\psi} + R\sin\theta\dot{\phi}^2 + L\cos^2\phi\dot{\psi}^2 - L\cos^2\theta\dot{\phi}^2 \\ +L\cos^2\theta\dot{\psi}^2 - L\cos^2\phi\cos^2\theta\dot{\psi}^2 + 2L\cos\phi\dot{\psi}\dot{\theta} + D\cos\phi\sin\theta\dot{\psi}^2 + R\cos\phi\cos\theta\ddot{\psi} \\ +H\cos\phi\sin\theta\ddot{\psi} + R\cos^2\phi\sin\theta\dot{\psi}^2 - 2R\cos\theta\sin\phi\dot{\phi}\dot{\psi} - 2L\cos\theta\sin\phi\sin\theta\dot{\phi}\dot{\psi} \end{bmatrix} \tag{1}$$

Passenger acceleration in the standard passenger frame P (x forward, y left, z up) is obtained from the above by rotating -pi/2 about the z-axis of frame 3:

$$a_P^{PO} = \begin{bmatrix} r\ddot{\psi}(H - L\cos\theta)\sin\phi + \ddot{\phi}(R + L\sin\theta) + \dot{\psi}^2\{D + R\cos\phi + L\cos\phi\sin\theta\}\sin\phi \\ +2\dot{\psi}\dot{\theta}L\sin\phi\sin\theta + 2\dot{\phi}\dot{\theta}L\cos\theta \\ \\ \ddot{\theta}L + \ddot{\psi}((L - H\cos\theta)\cos\phi + (D + R\cos\phi)\sin\theta) \\ -\dot{\psi}^2((H - L\cos\theta)\sin\theta + D\cos\phi\cos\theta + (R + L\sin\theta)\cos^2\phi\cos\theta) \\ -\dot{\phi}^2(R + L\sin\theta)\cos\theta + 2\dot{\psi}\dot{\phi}(-L\sin\phi + L\cos^2\theta\sin\phi - R\sin\phi\sin\theta) \\ \\ \ddot{\psi}((D + R\cos\phi)\cos\theta + H\cos\phi\sin\theta) + \dot{\theta}^2 L \\ +\dot{\psi}^2(-H\cos\theta + L(1 - \sin^2\phi\sin^2\theta) + (D + R\cos\phi)\cos\phi\sin\theta) \\ \dot{\phi}^2(R + L\sin\theta)\sin\theta + 2\dot{\psi}\dot{\theta}L\cos\phi - 2\dot{\psi}\dot{\phi}(R + L\sin\theta)\cos\theta\sin\phi \end{bmatrix} \tag{2}$$

The expression for gravitational acceleration in passenger frame P (added to point mass accelerations for retrieving 'experience G force passenger'):

$$g^P = g\begin{bmatrix} -\sin\psi\sin\phi \\ \cos\psi\sin\theta + \sin\psi\cos\phi\cos\theta \\ \cos\psi\cos\theta - \sin\psi\cos\phi\sin\theta \end{bmatrix} \tag{3}$$

Passenger G-force:

$$G_{eq}^P = \begin{bmatrix} -\sin\psi\sin\phi \\ 0 \\ \frac{\Omega^2}{g}(R + L\sin\theta_{eq})\sin\theta_{eq} + \cos\psi\cos\theta_{eq} - \sin\psi\cos\phi\sin\theta_{eq} \end{bmatrix} \tag{4}$$

B Simscape diagram model

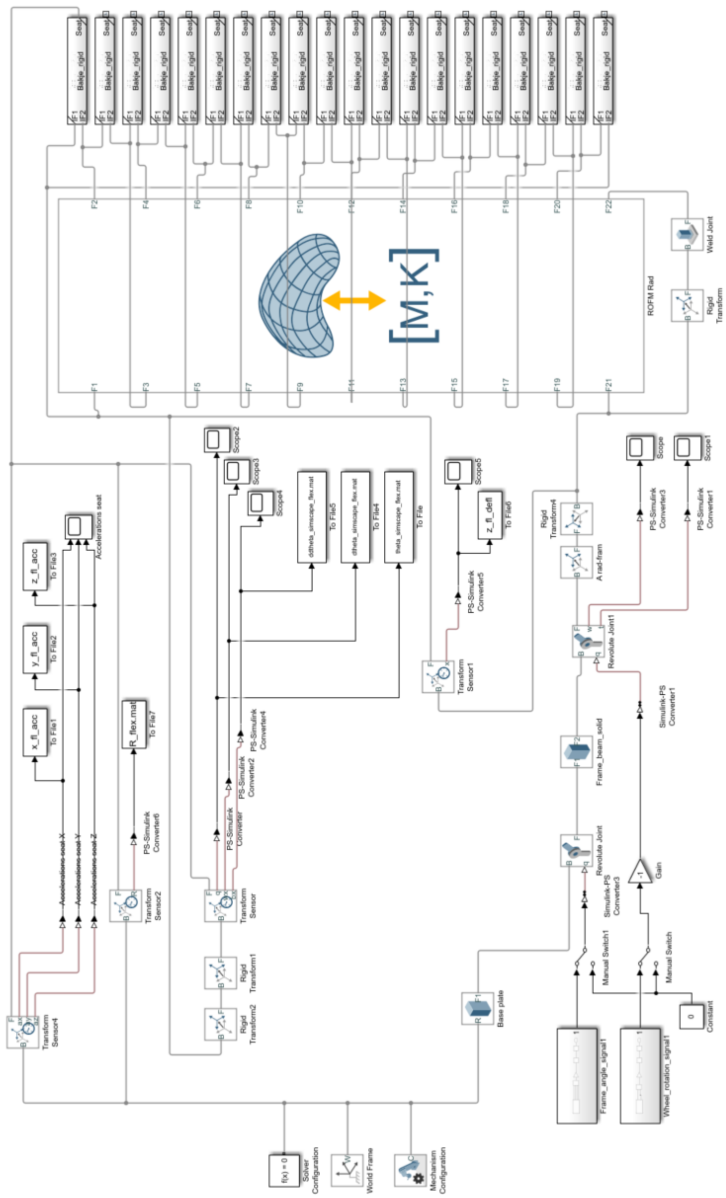

Figure 1: Flexible multibody model overview in SIMSCAPE, the rigid multibody model is very similar to this, but the Reduced Order Flexible Model is replaced by rigid transformation blocks.

C Experimental verification

Experimental verification of the Finite element model is conducted at the physical Enterprise present in Avonturenpark Hellendoorn, the Netherlands. The paper roughly describes the process and results, of which additional results and details are presented in this section.
The measurements are performed with a set of four accelerometers, which are attached to the Enterprise wheel frame by use of a magnetic mount. They are evenly spaced over 4 of the radial booms, close to the interface point between the frame and gondola. The sensors mounted in the experiment are visible in figure 2.
Excitation of the frame is done trough an impulse force on one of the radial booms, by jumping on it with full body weight. Measurement data is saved at a sample rate of 128 Hz for approximately 60 seconds. Analyzing the results and performing Fourier transform, results in the frequency domain. This methodology is conducted numerous times over different locations of the accelerometers and excitations. In general, with a few exceptions, the experiments brought similar results. One representative case is further treated, for which the locations of the accelerometers and excitation location are visible in figure 3.

(a) Acceleration sensor mount position

(b) Acceleration sensor mounted at the interface point of the central frame

Figure 2

For analysis of the mode shapes, the signals of all four sensors are first filtered around the observed eigenfrequencies from the frequency response. The phase differences in the data of different sensors is studied in detail. Together with knowledge of the sensor locations and the expected mode shapes it is able to deduct the mode shapes of the measured eigenmodes. For the representative case, this data is visible in figure 4.

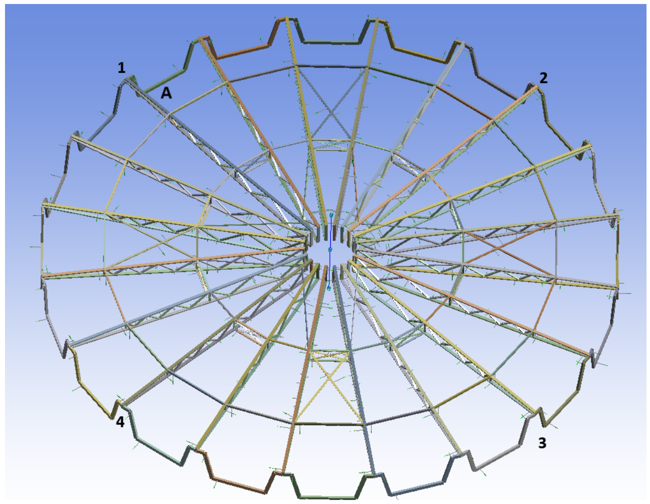

Figure 3: Sensor positions(1,2,3,4) and impulse actuation point(A) during experimental verification.

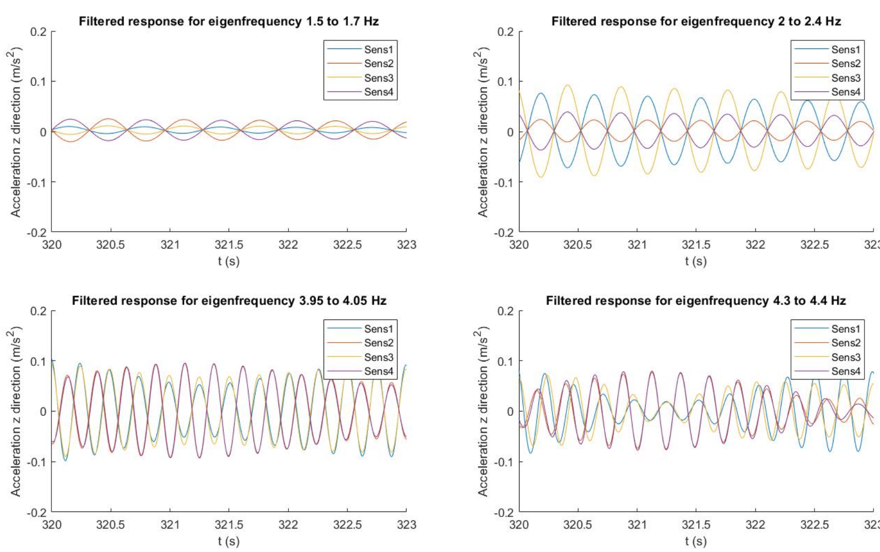

Figure 4: Measurement data for filtered frequency of natural modes, to determine mode shapes.